Kasetsart J. (Nat. Sci.) 43 : 411 - 421 (2009)

Reference Input Shaping to Reduce the Move Time of a Very Flexible One-Link Manipulator

Withit Chatlatanagulchai[1]*, Tanapon Srivongsa[1] and Peter H. Meckl[2]

ABSTRACT

When a robot manipulator is required to be light, long or to move quickly, its link tends to flex. When the link flexes, its end position is difficult to control. In fact, the flexibility brings about undesirable attributes such as non-minimum phase, tip vibration and complicated dynamics. As a result, in contrast to a rigid-link robot, control of the flexible-link robot is more challenging and is still an open research problem. This study aimed to design a two-degrees-of-freedom control system from a simple model. The controller ensured good tracking and proper disturbance rejection. The closed-loop natural frequency was then computed, with the reference input shaped such that its energy content was low around the natural frequency. The experiment showed that this proposed method reduced tip vibration significantly resulting in a faster move time.

Key words: vibration reduction, flexible link, command shaping, shaped reference inputs, quantitative feedback

INTRODUCTION

Space station activities in the 1980's spurred interest in the control of the flexible-link robot. A long boom in space must be light, long and accurately positioned and its link must be flexible. Since the application of the well-understood control of a rigid-link robot is not appropriate, researchers have had to find new and effective control and modeling methods.

Over the past three decades, the emerging industrial trend for lighter and faster robots with a higher payload capacity has resulted in tremendous efforts being spent in modeling and control as well as other areas such as structural optimization and sensor and actuator electronics. Nevertheless, an effective control that can be applied to all situations has not been found.

Modeling of the flexible-link robot can be divided into approximated and exact methods. Hastings and Book (1987) were among the first to propose an approximated model from the assumed modes approach. Interesting comment about the limitation of this approach has been given by Wang and Vidyasagar (1989). Jen *et al*. (1996) proposed a low-order transfer function from the Rayleigh-Ritz method, and Krishnan and Vidyasagar (1998) proposed a reduced-order model based on the Hankel-norm minimization.

The exact method, although not suitable for control design, describes the behavior of the robot more accurately. The model from the Euler-

1 Control of Robot and Vibration Laboratory (CRV Lab), Department of Mechanical Engineering, Faculty of Engineering, Kasetsart University, Bangkok 10900, Thailand.

2 School of Mechanical Engineering, Purdue University, West Lafayette, IN 47907-2088, USA.

* Corresponding author, e-mail: fengwtc@ku.ac.th

Received date : 02/12/08 Accepted date : 16/03/09

Bernoulli beam theory was derived in the work of Bellezza *et al*. (1990), Low (1997), and Iemsamai and Chatlatanagulchai (2008). The last work compared the exact model with an approximated model.

The majority of flexible-link robot controls use active methods, where external energy is provided to the system to control its response. Examples that used fixed models include that of Chapnik *et al*. (1993), whose controller was an open-loop computed torque, Jnifene and Fahim (1997), in which delayed deflection was added to counteract the non-minimum phase effect, and Baicu *et al*. (1998), where a nonlinear controller based on the backstepping approach was applied. Examples that used adaptive schemes have been given by Carusone *et al*. (1993), Konno and Uchiyama (1995), Moudgal *et al*. (1994), Yang *et al*. (1997), and Caswara and Unbehauen (2002), where methods such as gain scheduling, fuzzy logic, adaptive control and neuro-fuzzy control were applied.

Passive methods include traditional adjustment of spring and damping constants and reference input shaping, where the input is altered so less energy is injected around the natural frequency. The latter can be divided into two schemes. The first is based on the convolution of the reference input with a sequence of impulses. This scheme was proposed by Singer and Seering (1990). It was improved in the work of Tzes and Yurkovich (1993), Khorrami *et al*. (1995) and Mohamed and Tokhi (2004). Zuo and Wang (1992) pointed out the limitations of the first scheme, regarding bandwidth and frequency reproduction.

The second scheme used optimization setting. As proven by Meckl (1988), the amplitude of the residual vibration is directly proportional to the input spectrum magnitude around the natural frequency. Therefore, a series representation can be formed to imitate the bang-bang acceleration profile and to reduce the spectrum energy around any desired frequency. Chatlatanagulchai *et al*. (2006) applied this technique to a two-link flexible-joint robot.

In this paper, a control system was designed from a simple model obtained from a system identification of an actual robot. Being simple, this third-order model had uncertainty. A robust controller and a prefilter was then designed using the quantitative feedback theory, whose details can be found in the work of Chatlatanagulchai *et al*. (2007) for the SISO case and Chatlatanagulchai *et al*. (2008) for the MIMO case. This type of control system can handle uncertainty by incorporating it in the loop shaping process. The natural frequency was then found from the closed-loop system. The command shaping proposed by Meckl (1988) was then applied to obtain a reference trajectory whose energy was reduced around the closed-loop natural frequency, resulting in less excitation and hence less vibration and significantly faster move time.

The methods section of this paper introduces a one-link flexible-link robot and describes how a simple robot model can be obtained. Control system design and simulation results are subsequently discussed, followed by determination of the closed-loop natural frequency and shaping of the reference input. The reference input is then applied to an actual robot in the CRV laboratory. The experimental set-up and results are given in the results section. The summary, unsolved parts of the problem, and new research directions are presented in the conclusions section.

METHODS

Obtaining a simple robot model

A flexible-link robot normally has settings as shown in Figure 1. For this paper, the interest was in controlling its tip position, so point P is at the payload. The output variable to be controlled is α, which consists of the base angle θ, obtained from the base optical encoder, and the

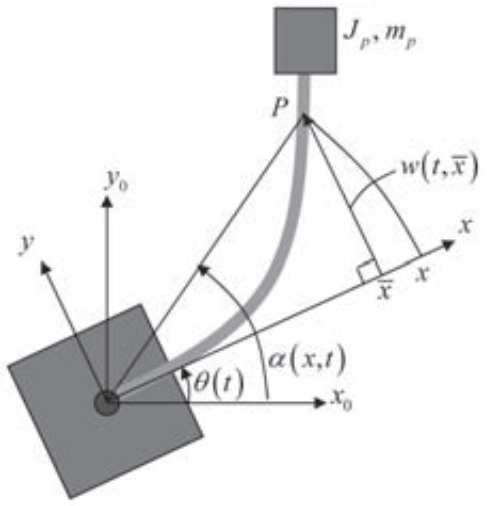

Figure 1 Diagram of a one-link flexible-link robot.

link angle, obtained from strain gauges attached along the flexible link. The goal is to move α so the link is moved from point to point with the least settling time possible.

Several frequency-varying sine signals were given as input voltage v to the robot. The output α was recorded. The input and output pairs were fitted together using Matlab's System Identification toolbox to produce several transfer functions. The experiment was repeated several times with a new set of input signals. As a result, a transfer function was obtained with good validation (Equation 1):

$$\frac{\alpha}{v} = P = \frac{1.128}{0.00264\ s^3 + 0.0656\ s^2 + 0.4649\ s + 1}, \quad (1)$$

with the validation results shown in Figure 2. Care was taken not to over-fit the model with any particular set of data.

Control system design and simulation

Having obtained the model, the control system was then designed (Figure 3), where α_d is the reference input. d_o is a disturbance at plant output, such as ground vibration, to be attenuated. G and F are the controller and prefilter.

The plant P is given in , with each parameter allowed to deviate by ± 10%, based on performing several system identifications. On the Nichols chart, the so-called plant templates $\{P\}$ were plotted at pertaining frequencies. Figure 4 shows the plant templates at five frequencies, where asterisks mark nominal positions.

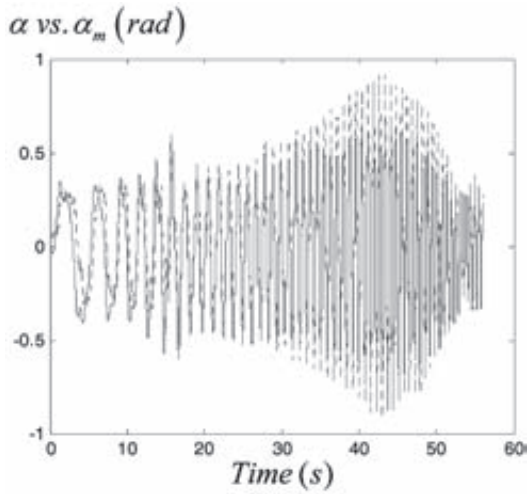

Figure 2 Robot model validation. The solid line is the model output; the dotted line is the actual output.

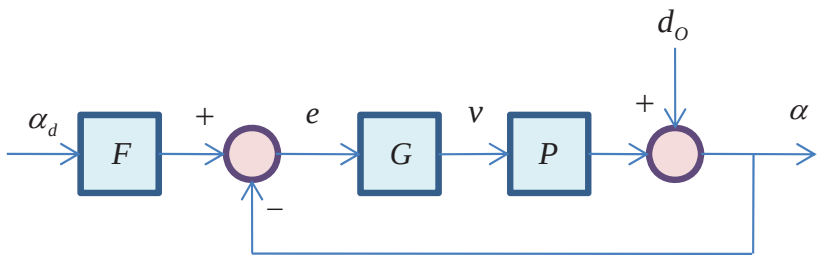

Figure 3 Diagram of a feed-forward/ feedback system.

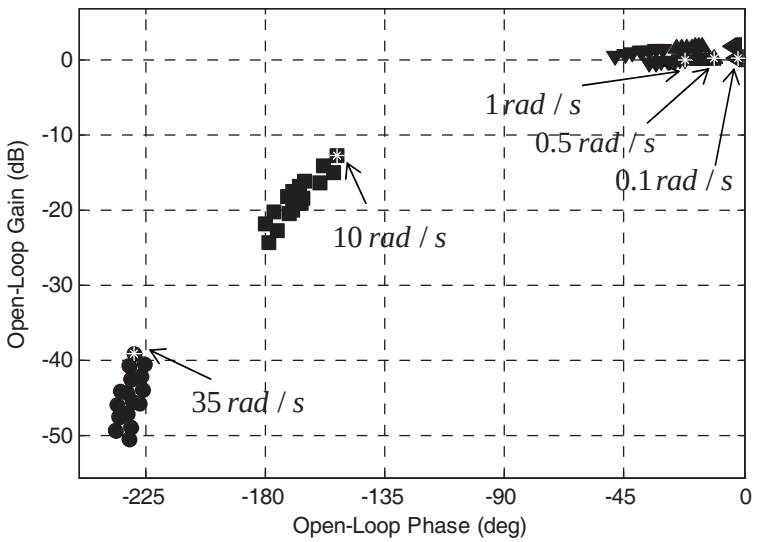

Figure 4 Plant templates at various frequencies.

The control system was designed to achieve good tracking, stability and disturbance attenuation. As a result, two specifications were set in the frequency domain, as Equation 2:

$$\left|\frac{1}{1+GP}\right| < \delta_s \qquad (2)$$

and Equation 3:

$$\delta_{LB} < \left|\frac{FGP}{1+GP}\right| < \delta_{UB}, \qquad (3)$$

where $\delta_s = 4$ and δ_{LB} and δ_{UB} are two transfer functions:

$$\delta_{LB} = \frac{3.92}{s^2 + 4s + 4}$$

and:

$$\delta_{UB} = \frac{16.32}{s^2 + 8s + 16},$$

with each having suitable step responses. Equation is for tracking and it is easy to show that Equation ensures good stability and plant-output disturbance attenuation.

Specifications were converted into bounds on the Nichols chart. When each bound was drawn, all points in the corresponding plant template were incorporated to ensure that the resulting controller, designed in the next step, would be robust for all possible plant variations in the template.

Two bounds, for and were obtained for each frequency. The two bounds were combined and the stricter portion was selected to create the worst-case bound. Figure 5 contains five worst-case bounds for five selective frequencies.

In the loop-shaping step, the controller G was designed, such that the resulting open-loop shape $L = GP$ lies in an acceptable region. Figure 5 shows the open-loop shape after the loop shaping. The controller is in the form:

$$G = \frac{(2s+1)}{s}$$

The prefilter is trivial and is left as $F = 1$.

Figure 6 shows the simulation results. Each solid line in the pack represents the simulation of a one-point plant in the template. In Figure 6a, the specification is the dotted line, whereas the asterisks mark the designed frequencies. It can be seen that specification is met for all possible plant variations.

Figure 6b shows the tracking result, which falls out of the bounds only at high frequencies, the region not included in the design

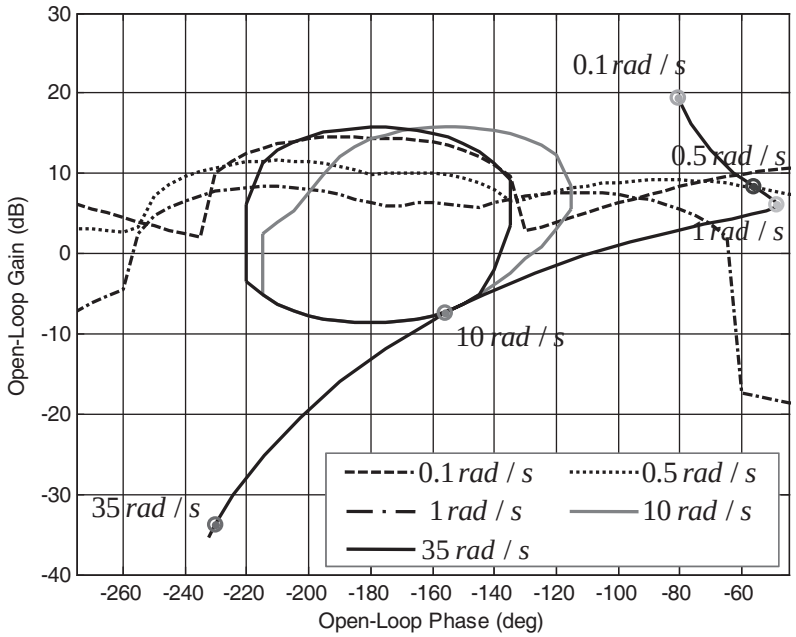

Figure 5 QFT worst-case bounds and open-loop shape.

to avoid noise. Figure 6c plots the output α when the step disturbance d_o was applied and it can be seen that the disturbance is appropriately attenuated.

Figure 6d contains the tracking result, where *LB* and *UB* are two time-domain bounds obtained from passing a square wave α_d into the transfer functions δ_{LB} and δ_{UB}. The simulated output α was able to follow its desired α_d within the bounds most of the time for all plant variations.

Shaping of the reference input

The natural frequency of the closed-loop system can be computed. For the nominal closed-loop system, it is 8 *rad* / *s*.

The reference input for the robot to follow can be obtained from integrating the bang-bang acceleration profile. Figure 7 shows the bang-bang acceleration profile as well as its resulting reference velocity and position. It can be seen from Figure 7b that the reference input spectrum amplitude is high over the natural frequency 8 *rad* / *s*.

As mentioned by Meckl (1988), there is a direct relationship between the magnitude of the input spectrum at the natural frequency and the amplitude of the residual acceleration. It is considered certain that inputting this reference input would result in a high level of residual vibration.

To improve the situation, the work of Meckl (1988) was followed by shaping the reference input so that its energy content was lower around 8 *rad* / *s* using the fact that any input function can be represented by the series:

$$f(t) = \sum_{l=1}^{L} \frac{B_l}{\alpha_l^2} \Phi_l^*(t), \tag{4}$$

where B_l is the coefficient for each harmonic and:

$$\Phi_l^*(t) = \alpha_l \left(\frac{1}{2} - \frac{t}{T_f} \right) + \sin \alpha_l \frac{t}{T_f} - \frac{\alpha_l}{2} \cos \alpha_l \frac{t}{T_f}$$

is a ramped sinusoidal function with α_l as a characteristic number associated with each harmonic and as move time.

B_l can be chosen to minimize the cost function:

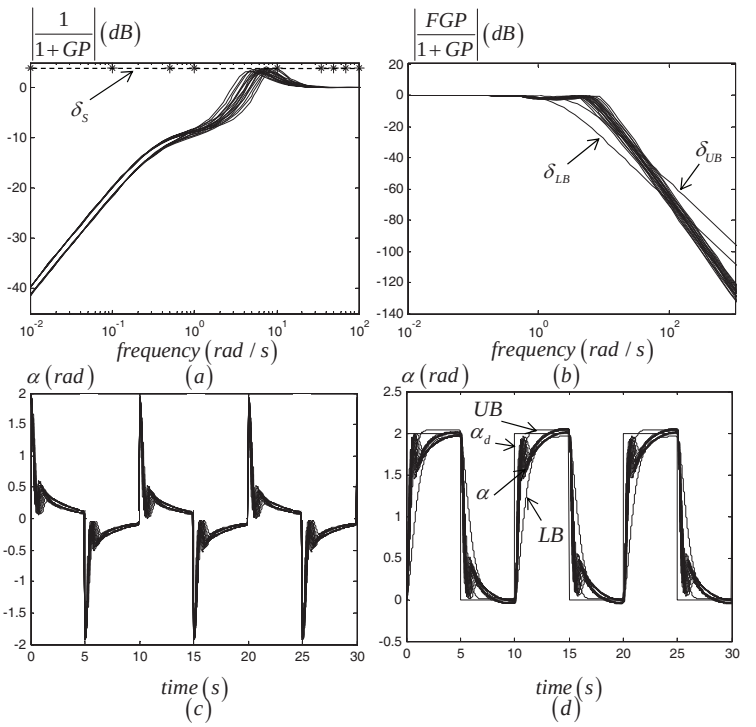

Figure 6 Simulation results: (a) stability; (b) tracking; (c) disturbance rejection; (d) tracking in the time domain.

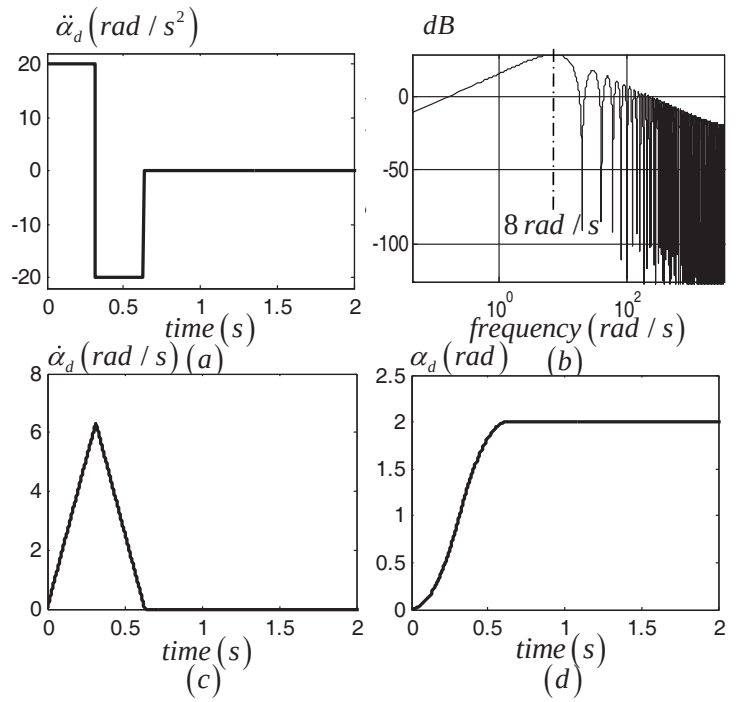

Figure 7 Square-wave reference inputs: (a) reference acceleration $\ddot{\alpha}_d$; (b) frequency spectrum of $\ddot{\alpha}_d$; (c) reference velocity $\dot{\alpha}_d$; (d) reference position α_d.

$$J = \frac{1}{T_f}\left\{\int_0^{T_f/2}\left[1 - f(t)\right]^2 dt + \int_{T_f/2}^{T_f}\left[-1 - f(t)\right]^2 dt\right\}$$

$$+ \rho\sum_{i=1}^{11}(\omega_i T_s)^2\left|F^*(\omega_i T_f)\right|^2, \qquad (5)$$

where ρ is a relative weighting between two objectives – the first term to mimic the bang-bang profile for a fast move, the second term to lower the energy content around ω_n – and T_s is the move time to cover a distance y_f when the input is a single cycle of a square wave of amplitude $F_{\max}$. The cost function contains 11 frequencies surrounding resonance; this number can be changed arbitrarily. In this case, ± 10% deviation from $\omega_n = 8$ *rad / s* was used, with the bounds on the frequency ω_i being $0.9\omega_n < \omega_i < 1.1\omega_n$. The percent deviation was computed from each plant in the plant template.

It was possible to construct $\ddot{\alpha}_d$ using the series (4). The cost function was minimized using the design parameters: $L = 20$, $\rho = 1$, $\omega_n = 8$ *rad / s*, and $F_{\max} = 20$. The desired move distance was $y_f = 2$ *rad*. Figure 8a shows the shaped $\ddot{\alpha}_d$ together with its frequency spectrum in Figure 8b. The spectrum magnitude around the natural frequency was greatly reduced. Time plots of the corresponding $\dot{\alpha}_d$ and α_d are given in Figure 8c and 8d.

Note that the desired move time increased from 0.67 *s* in the square-wave case (Figure 8d) to 1.42 *s* in the ramped sinusoidal case (Figure 8c). This was due to the fact that the energy was pulled out from the spectrum around the natural frequency resulting in a slower, desired position profile. However, as can be seen in the experimental results, the ramped sinusoidal profile greatly reduced the robot's move time because it induced a lot less residual vibration than the square-wave profile.

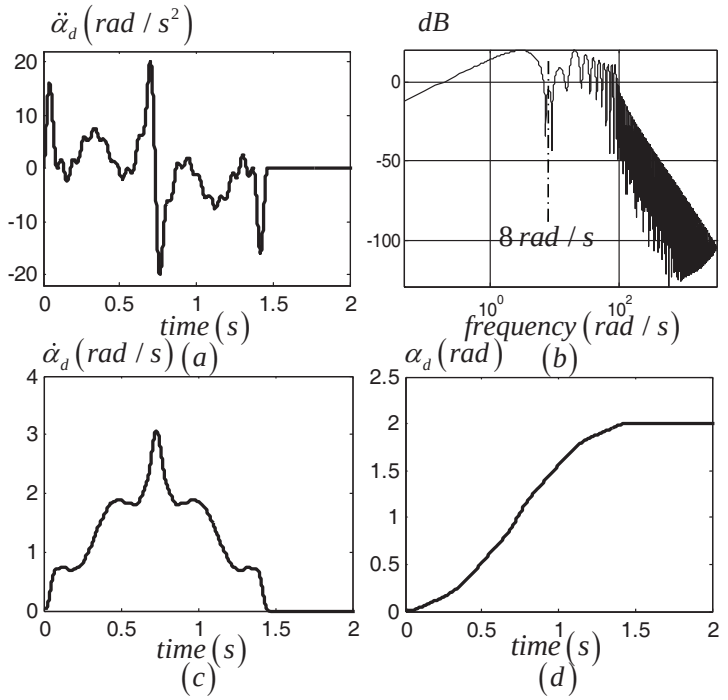

Figure 8 Shaped reference inputs: (a) reference acceleration $\ddot{\alpha}_d$; (b) frequency spectrum of $\ddot{\alpha}_d$; (c) reference velocity $\dot{\alpha}_d$; (d) reference position α_d.

RESULTS

Experimental set-up and results

Figure 9 shows a photograph of the flexible-link robot. An accelerometer was mounted with the payload located at the tip. Three strain gauges were used to measure transversal deflection, and an optical encoder was used to measure motor and hub angle. A steel ruler was used as the flexible link with an effective length of 0.54 *m*.

Figure 10 shows a block diagram of the experimental arrangement. A host computer, with necessary software, was used to communicate with the user and a target computer. The target computer contained a data acquisition card whose functions were to acquire sensor signals and to send out actuator commands from the control algorithm. The host and target computers were connected to each other via a LAN line. A control signal was

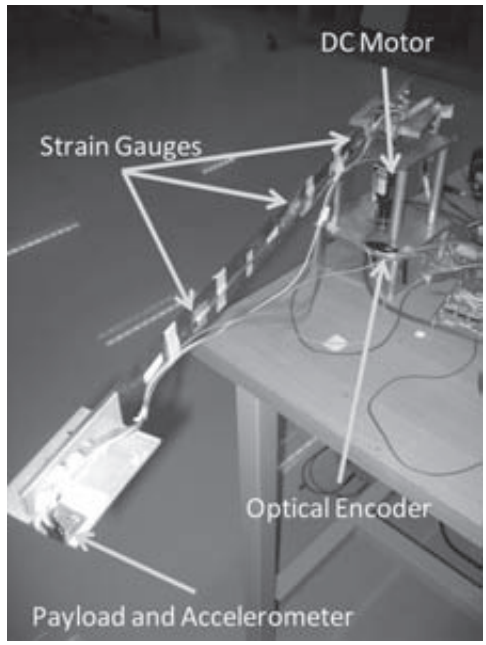

Figure 9 Photograph of the flexible-link robot in the laboratory.

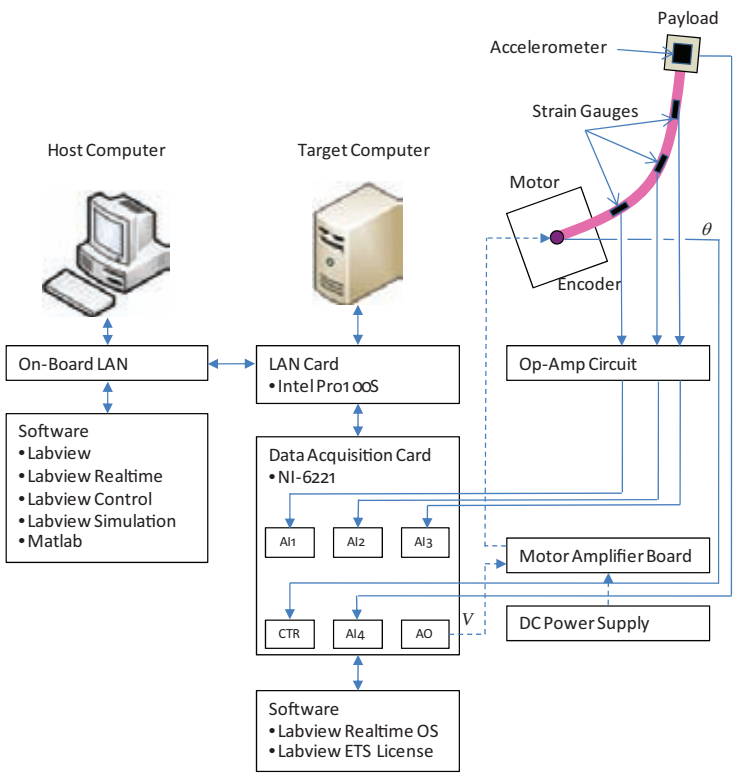

Figure 10 Block diagram of the experimental set-up and associated hardware.

sent as voltage to a motor amplifier board to amplify to a level that can drive the DC motor. An IC chip accelerometer was mounted at the tip to measure linear acceleration. An in-house-design op-amp circuit amplified and filtered signals from the strain gauges. A DC power supply supplied the required current to the motor amplifier board.

A sampling time of 1 *ms* was used for the hardware and for discretizing the controller. A switch was made in the program to alternate between supplying the shaped reference input and the unshaped (bang-bang) reference input. Figure 11a plots the robot's tip position α versus its desired square-wave trajectory α_d. By alternating between the shaped and unshaped reference inputs, it can be clearly seen that, with the shaped input, the robot was able to move faster with significantly less settling time than in the unshaped case, which suffered from severe residual vibration.

Figure 11b shows the signals from the accelerometer at the tip, with significantly higher acceleration output seen during the unshaped periods.

CONCLUSIONS

With shaping of the reference input, the flexible-link robot achieved faster point-to-point motion due to less residual vibration. Not only could the robot be operated faster, but also with less vibration that reduced damage to both the robot and its payload. The algorithm presented in this paper is easy to implement, requiring only information on the natural frequencies of the system.

The unsolved part of the algorithm was that the shaped input could only be obtained off-line. Therefore, the robot path must be pre-specified. Although this works well for repetitive robots like those in industries, the algorithm will not work for a robot with unknown or adaptive paths. More research should be carried out to develop an on-line algorithm.

ACKNOWLEDGEMENTS

The first author would like to thank Craig Borghesani and Terasoft, Inc for their evaluation copy of the QFT toolbox. This work was carried out at the Control of Robot and Vibration Laboratory, which is situated at and partially supported by the Research and Development Institute of Production Technology (RDiPT) of Kasetsart University, Thailand. This work was also sponsored by graduate-level research funding from the Graduate School of Kasetsart University, Thailand.

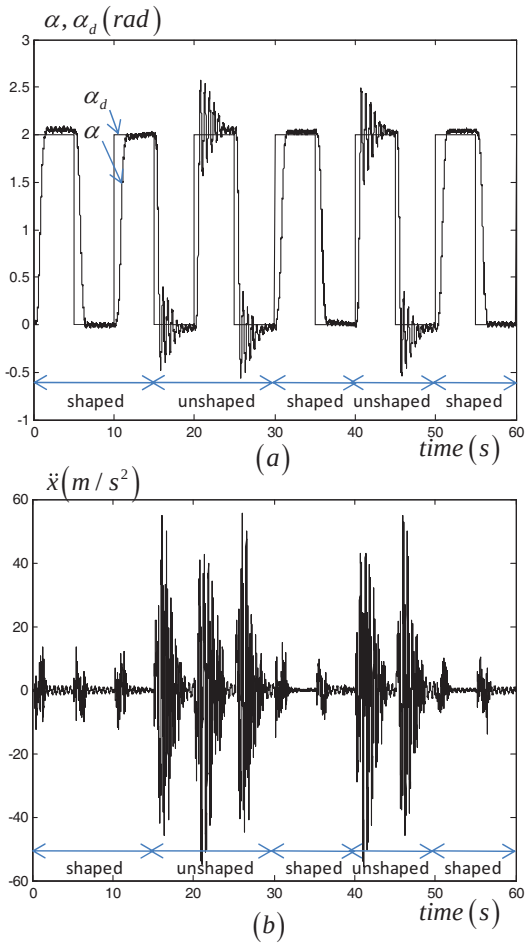

Figure 11 Experimental results for shaped and unshaped cases: (a) angular position output α and its desired value α_d; (b) tip acceleration $\ddot{x}$.

LITERATURE CITED

Baicu, C.F., C.D. Rahn and D.M. Dawson. 1998. Backstepping boundary control of flexible-link electrically driven gantry robots. **IEEE Trans. Mechatron**. 3(1): 60-66.

Bellezza, F., L. Lanari and G. Ulivi. 1990. Exact modeling of the flexible slewing link, pp. 734-739. *In* **Proc. IEEE Int. Conf. on Robotics and Automation** Cincinnati. Ohio.

Carusone, J., K.S. Buchan and G.M.T. D'Eleuterio. 1993. Experiments in end-effector tracking control for structurally flexible space manipulators. **IEEE Trans. on Robotics and Automation** 9(5): 553-560.

Caswara, F.M. and H. Unbehauen. 2002. A neurofuzzy approach to the control of a flexible-link manipulator. **IEEE Trans. on Robotics and Automation** 18(6): 932-942.

Chapnik, B.V., G.R. Heppler and J.D. Aplevich. 1993. Controlling the impact response of a one-link flexible robotic arm. **IEEE Trans. on Robotics and Automation** 9(3): 346-351.

Chatlatanagulchai, W., V.M. Beazel and P.H. Meckl. 2006. Command shaping applied to a flexible robot with configuration-dependent resonance, pp. 1766-1711. *In* **Proc. of the 2006 American Control Conf.** Minneapolis. MN.

Chatlatanagulchai, W., B. Inseemeesak and W. Siwakosit. 2007. Quantitative feedback control of a pendulum with uncertain payload. **J. Research in Engineering and Technology** 4(4): 347-367.

Chatlatanagulchai, W., C. Srinangyam and W. Siwakosit. 2008. Trajectory control of a two-link robot manipulator carrying uncertain payload using quantitative feedback theory. **J. Research in Engineering and Technology** 5(1): 45-71.

Hastings, G.G. and W.J. Book. 1987. A linear dynamic model for flexible robotic manipulators. **IEEE Contr. Syst. Mag.** 61-64.

Iemsamai, K. and W. Chatlatanagulchai. 2008. Exact mathematical model of the flexible-link robot, pp. 399-404. *In* **Proceedings of the 22nd ME-NETT.** Patumthani. Thailand.

Jen, C.W., D.A. Johnson and R. Gorez. 1996. A reduced-order dynamic model for end-effector position control of a flexible robot arm. **Math. Comput. Simul.** 41: 539-558.

Jnifene, A. and A. Fahim. 1997. A computed torque/time delay approach to the end-point control of a one-link flexible manipulator. **Dynamics and Control** 7: 171-189.

Khorrami, F., S. Jain and A. Tzes. 1995. Experimental results on adaptive nonlinear control and input preshaping for multi-link flexible manipulators. **Automatica** 31(1): 83-97.

Konno, A. and M. Uchiyama. 1995. Vibration suppression control of spatial flexible manipulators. **Control Eng. Practice** 3(9): 1315-1321.

Krishnan, H. and M. Vidyasagar. 1998. Control of single-link flexible beam using Hankel-norm-based reduced-order model. **IEE Proc. Control Theory Appl**. 145(2): 151-158.

Low, K.H. 1997. A note on the effect of hub inertia and payload on the vibration of a flexible slewing link. **J. Sound and Vibration** 204(5): 823-828.

Meckl, P.H. 1988. **Control of Vibration in Mechanical Systems Using Shaped Reference Inputs**. PhD Thesis. Department of Mechanical Engineering. Massachusetts Institute of Technology.

Mohamed, Z. and M.O. Tokhi. 2004. Command shaping techniques for vibration control of a flexible robot manipulator. **Mechatronics** 14: 69-90.

Moudgal, V.G., K.M. Passino and S. Yurkovich. 1994. Rule-based control for a flexible-link robot. **IEEE Trans. on Cont. Sys. Tech**. 2(4): 392-405.

Singer, N.C. and W.P. Seering. 1990. Preshaping command inputs to reduce system vibration.

ASME Trans. J. Dynam., Meas., Contr. 112(1): 76-82.

Tzes, A. and S. Yurkovich. 1993. An adaptive input shaping control scheme for vibration suppression in slewing flexible structures. **IEEE Trans. on Control Syst. Technol.** 1(2): 114-121.

Wang, D. and M. Vidyasagar. 1989. Transfer function for a single flexible link. **IEEE Int. Conf. on Robotics and Automation** 1042-1047.

Yang, J.H., F.L. Lian and L.C. Fu. 1997. Nonlinear adaptive control for flexible-link manipulators. **IEEE Trans. on Robotics and Automation** 13(1): 140-148.

Zuo, K. and D. Wang. 1992. Closed loop shaped-input control of a class of manipulators with a single flexible link. pp. 782-787 In. **Proc. of the 1992 IEEE Int. Conf. on Robotics and Automation** Nice. France.